Polarized measurements of spectrally narrowed emissions from a single crystal of a thiophene/phenylene co-oligomer

Takeshi Yamao,[a] Takayuki Ohira, Satoshi Ota, and Shu Hotta
Department of Macromolecular Science and Engineering, Kyoto Institute of Technology, Matsugasaki, Sakyo-ku, Kyoto 606-8585, Japan

(Received 5 December 2006; accepted 21 February 2007; published online 25 April 2007)

The spectrally narrowed emissions (SNE) from a flat single crystal of a thiophene/phenylene co-oligomer were investigated in a series of polarized measurements. The SNE spectra comprise of two major lines occurring at 507 and 514 nm. Of these, the former line effectively causes the emission gain narrowing by the pulse laser excitation polarized along the *c* axis. The intensity of the SNE is nearly isotropic with the radial directions along the flat crystal plane paralleling the *bc* plane. The SNE is strongly polarized along the *a* axis with its emission polarization ratio of the *a* axis to the *b* axis being 16.7. These polarized SNEs can be understood by the upright configuration of the molecular long axis paralleling the *a* axis. © *2007 American Institute of Physics*.
[DOI: 10.1063/1.2719011]

I. INTRODUCTION

Organic semiconducting materials have been drawing increasing attention over the past decade thanks to their excellent optoelectronic properties. In particular, conjugated molecules and polymers have large potential as useful materials for optical devices. As an example spectrally narrowed emissions (SNE), such as the laser oscillation and amplified spontaneous emission (ASE), are observed through photoexcitation of those crystals.[1,2] The conjugated molecular crystals, in turn, exhibit good charge transport characteristics in device configurations such as field-effect transistors.[3–11] Thus, the integrated features regarding optics and electronics make these conjugated molecular crystals very attracting and promising. With these circumstances as a background, recently, thiophene-based molecular semiconductors show particularly interesting features. Fichou *et al.*[12] and Horowitz *et al.*[13] first demonstrated the SNE from oligothiophenes in the form of single crystals. Nagawa *et al.*,[14] Hibino *et al.*,[15] Ichikawa *et al.*,[16] and Shimizu *et al.*[17] also observed the SNE using a variety of thiophene/phenylene co-oligomers (TPCOs). They attributed the relevant SNE to the ASE. Very recently the laser oscillation has definitively been confirmed using single crystals of TPCOs.[18,19]

In the present studies we have investigated the SNEs from a single crystal of a TPCO material of BP1T-OMe [see the structural formula in Fig. 1(a) and a photograph of its crystal in Fig. 1(b)]. Flat crystals of BP1T-OMe show strong emissions from the crystal edges and the SNE can be observed under strong laser light excitation as in the case of other thiophene-based oligomers.[12–19] Using these crystals we measured emissions in various directions along the flat crystal plane. Polarized emissions were studied as well. For the purpose of the present studies we grew in vapor phase single crystals of BP1T-OMe and carefully chose from among them one of ~1.0 mm in length, 0.46 mm in width, and ~630 nm in thickness [see Fig. 1(b)]. We determined the crystal axes as in Fig. 1(b) from a polarized micrograph observation and characteristic angles of the crystal.[20] The *c* axis is parallel to the crystal long side and the *a* axis is perpendicular to the flat crystal plane (i.e., the *bc* plane). The three crystal axes are orthogonal to one another. This geometrical feature enables us to carry out the polarized spectroscopic measurements relative to the mentioned crystal axes. The emissions are highly polarized parallel to the normal of the flat crystal plane. This is principally because the crystals belong to an orthorhombic system, producing a rigorously upright configuration of the molecular long axis against the crystal plane.[20] Here the molecular long axis is defined as the line connecting the two oxygen atoms. This renders the BP1T-OMe exceptionally suited to the polarized spectroscopic studies.

II. EXPERIMENTS

The synthesis and purification methods can be seen elsewhere.[21] The crystals of BP1T-OMe were grown by us-

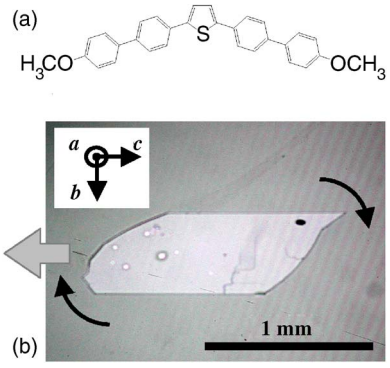

FIG. 1. (a) Structural formula of BP1T-OMe. (b) Micrograph of the BP1T-OMe crystal. A series of measurements was routinely started from this configuration where the crystal was placed with the *c* axis horizontal. We detected the emission occurring from the left parts of the crystal as indicated with a thick arrow. As an option of measurements the crystal was rotated around the normal to the crystal plane as indicated with a pair of arced arrows.

[a]Electronic mail: yamao@kit.ac.jp

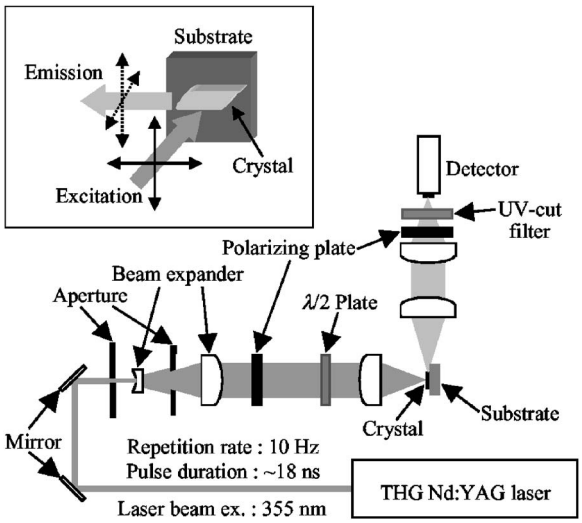

FIG. 2. Schematic diagram of experimental setup for the emission measurements. The inset shows an enlarged measurement geometry where different excitation and emission polarization directions are indicated.

ing the sublimation recrystallization method. Our apparatus and growth method are based mainly upon those described in the previous literature.[22–24] The apparatus consists of a glass tube and two closely aligned band heaters wound around the tube. The first heater is set at a high temperature for sublimation and the second one is for crystallization. The BP1T-OMe powder was placed in the glass tube under a N_2 gas flow (55 ml/min) at normal pressure and heated up to 360 °C by the first heater. After 6 h heating crystals were grown on the inner wall of the glass tube close to the second heater (310 °C). The single crystal shown in Fig. 1 was chosen from among them and mounted on a glass substrate for the measurements.

The experimental setup for the polarized emission measurements is schematically shown in Fig. 2. The inset shows an enlarged measurement geometry where different excitation and emission polarization directions are indicated. The excitation light was incident perpendicular to the flat crystal plane. We detected the emission that occurred from the crystal edge and propagated parallel to the crystal plane. Thus we are measuring the emissions taking place in the direction vertical to the incident excitation light (see the inset of Fig. 2). The excitation laser light was rigorously polarized with a polarizing plate and the polarization direction was subsequently rotated with a half-wave plate. The laser beam was focused on the crystal plane so as to be from 2.4 to 3.4 mm in diameter to irradiate the whole crystal. As an option of measurements the glass substrate (on which the crystal was mounted) was manually rotated around the normal to the crystal plane [Fig. 1(b)]. This allows us to measure the emissions occurring from different parts of the crystal edge and propagating parallel with the crystal plane in varying radial directions.

For the excitation we used the third harmonic generation (355 nm) of a Nd:YAG laser (LOTIS TII, Nd:YAG Laser System LS-2137) to provide 18 ns pulses with a 10 Hz repetition rate. The excitation energy (per pulse) was calculated from average excitation power divided by both the irradiation area and the repetition rate and controlled using ND filters and a pair of concave and convex lenses which comprises of a beam expander. The emissions from the crystal were detected with a photonic multichannel analyzer (Hamamatsu Photonics, PMA11/C7473–36) after passing through a UV-cut filter. Another polarizing plate was placed just in front of the UV-cut filter to optionally examine the polarized emission.

TABLE I. Excitation polarization direction, sample rotation, emission polarization, and excitation laser energy for each experimental condition.

Condition	Excitation polarization direction	Sample rotation	Emission polarization	Excitation laser energy per pulse (μJ/cm^2)
1	*c* axis	No	No	5.5–551
2	*c* axis /*b* axis	No	*a* axis to *b* axis	347
3	*c* axis	Yes	No	587
4	*c* axis to *b* axis	Yes	No	587

III. RESULTS

The emission spectra comprise of two major lines occurring at 507 and 514 nm. The former (latter) line observed occasionally as a shoulder was located 506.3–507.8 nm (513.8–514.5 nm) at our instrumental resolution. We measured emissions from a BP1T-OMe single crystal with varying conditions. The following measurement conditions were adopted: (i) excitation geometry (i.e., the positional relationship between the excitation polarization direction and crystal axes) can be changed; (ii) various directions in which emissions take place can be changed. To achieve the conditions (i) and (ii), the excitation polarization direction and/or the crystal were rotated. (iii) Additionally the emissions were polarized just in front of the detector. Below we summarize experimental results according to these measuring conditions. Also see Table I for these conditions.

A. Condition 1 (the *c* axis polarized excitation without the sample rotation)

First, we observed the emission that was occurring from the same parts of the crystal; see a thick arrow in Fig. 1(b) indicating this emission direction. The excitation energies were varied from 5.5 to 551 μJ/cm^2. Except for Condition 1 we used the fixed energy for individual measurements (see Table I). The emission intensities were increased with increasing excitation energies, accompanied by the emission gain narrowing. The two lines peaking at 507 and 514 nm are involved. Of these, the former line can be noticed as a shoulder (around 69 μJ/cm^2 excitation), but this line rapidly grows with larger excitation energies and dominates at 551 μJ/cm^2 excitation with full width at half maximum (FWHM) of 6.5 nm. Nonlinear increment of the emission intensity and a sudden decrease in FWHM are noted around an excitation energy of 300 μJ/cm^2. A series of nonpolarized emission spectra is displayed in Fig. 3. The intensity of the other line (at 514 nm), on the other hand, shows a weaker dependence on the excitation energies.

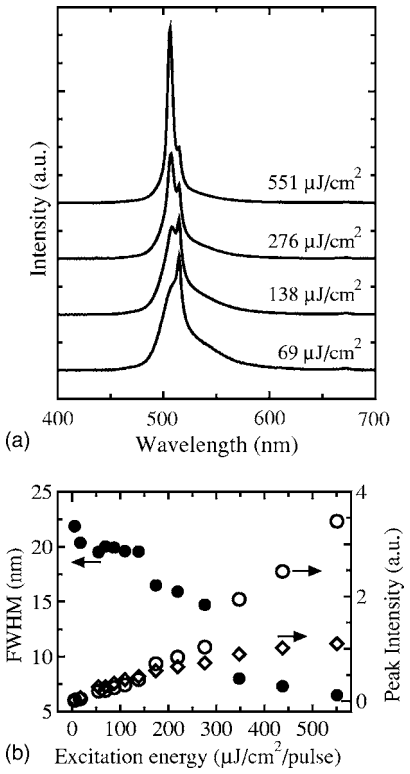

FIG. 3. (a) Nonpolarized emission spectra of the BP1T-OMe crystal excited with the *c* axis polarized light at various excitation energies (see Condition 1 in Table I). (b) Excitation energy dependence of peak intensity of the 507 nm line (open circles) and the 514 nm line (open squares). Full width at half maximum (FWHM) of the spectra are indicated with closed circles. The FWHM is determined from the overall spectrum; the same applied to the subsequent figures.

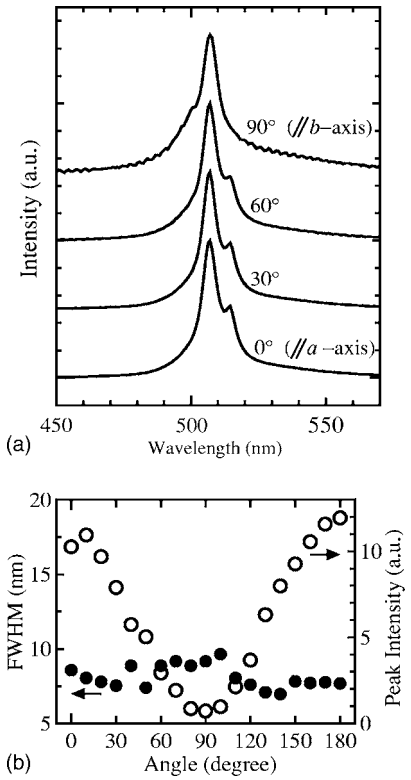

FIG. 4. (a) Polarized SNE spectra of the crystal excited with the *c* axis polarized light (Condition 2 in Table I). The angle between the polarizing plate (placed just in front of the detector) and the *a* axis was varied 0° −180°. The diagram shows the results of 0° (parallel to the *a* axis) to 90° (parallel to the *b* axis). (b) Peak intensity and FWHM as a function of the aforementioned angle.

We determined the FWHM from the overall spectrum by routinely taking a spectral width at the half of the largest emission intensity. In the stronger excitation regime the FWHM has been determined solely from the dominant 507 nm line.

B. Condition 2 (the *c* axis/*b* axis polarized excitation without the sample rotation)

Second, we investigated the emission polarization features. Since we have confirmed the occurrence of the gain narrowing around 300 $\mu J/cm^2$ of excitation, we measured the spectra at an energy above this (i.e., 347 $\mu J/cm^2$ excitation for Condition 2). Figures 4 and 5 show the results of the *c* axis and *b* axis excitation, respectively. In both cases the emissions are strongly polarized along the *a* axis. Their emission polarization ratios of the *a* axis to the *b* axis were both 16.7. For the *c* axis excitation, again, the 507 nm line dominates (with the 514 nm line as a shoulder); its FWHM was 7.0 nm (Fig. 4). This FWHM is significantly smaller than that in Fig. 5.

C. Condition 3 (the *c* axis polarized excitation with the sample rotation)

Third, we stepwise rotated both the excitation polarization and the crystal in the same direction and measured the nonpolarized emission spectra. As a result the excitation polarization direction was held parallel to the crystal *c* axis. The excitation energy was fixed at 587 $\mu J/cm^2$. In this case both the emission intensities and FWHM (~6 nm) of the dominant 507 nm line are kept roughly the same, even though fluctuation around the average could be noticed (Fig. 6). This clearly indicates that the intensities of emissions are nearly isotropic with the radial directions in parallel with the crystal plane.

D. Condition 4 (the *c* axis to *b* axis polarized excitation with the sample rotation)

We stepwise rotated the crystal and measured the nonpolarized emission spectra with the excitation polarization direction *unrotated*. As a result the excitation polarization direction was stepwise switched from the *c* axis to the *b* axis. The excitation energy was fixed at 587 $\mu J/cm^2$. The results are depicted in Fig. 7. When the excitation polarization direction is parallel to the *c* axis, the sharply resolved 507 nm line indicates a strong emission intensity (FWHM: 6.2 nm). For the *b* axis excitation the 507 nm line lessens its intensity and the FWHM becomes large. The 514 nm line, on the other hand, shows weaker dependence on the excitation polarization direction. The overall spectra were broadened and FWHM was ~20 nm at the *b* axis polarized excitation measurement.

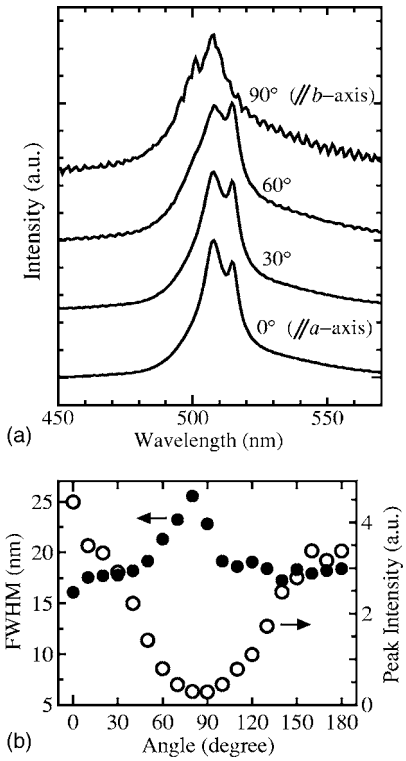

FIG. 5. (a) Polarized SNE spectra of the crystal excited with the *b* axis polarized light (Condition 2 in Table I). The angle between the polarizing plate and the *a* axis was varied 0°–180°. The diagram shows the results of 0°–90°. (b) Peak intensity and FWHM as a function of the aforementioned angle.

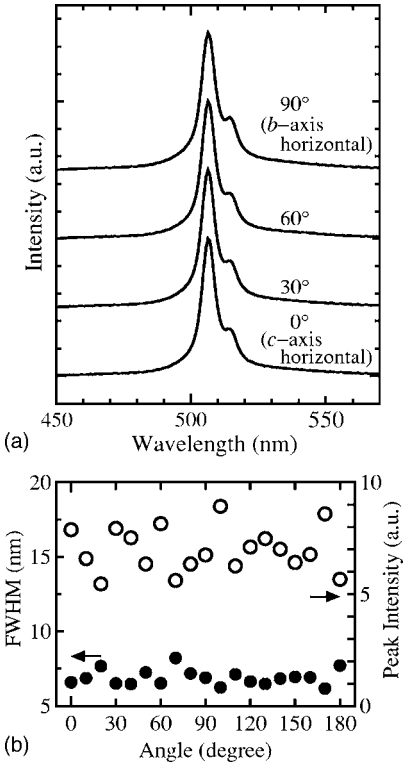

FIG. 6. (a) Nonpolarized SNE spectra of the crystal excited with the *c* axis polarized light (Condition 3 in Table I). The crystal was rotated stepwise (0°–180°) with the excitation polarization direction held parallel to the *c* axis. The diagram shows the results of 0° (for which the *c* axis is horizontal) to 90° (*b* axis is horizontal). (b) Peak intensity and FWHM as a function of the crystal rotation angle.

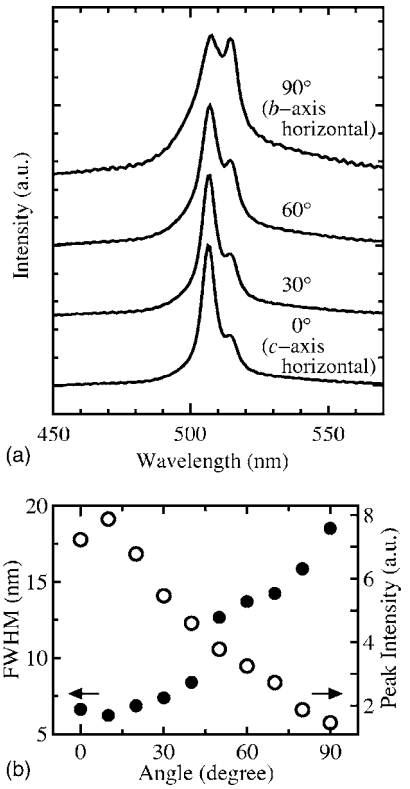

FIG. 7. (a) Nonpolarized emission spectra of the crystal excited with the varying polarized lights (Condition 4 in Table I). The crystal was rotated stepwise (0°–90°); the angle between the excitation polarization direction and the *c* axis was varied 0°–90°. (b) Peak intensity and FWHM as a function of the crystal rotation angle.

IV. DISCUSSION

The fact that the emissions are strongly polarized along the *a* axis under Condition 2 is a consequence of the upright configuration of the *a* axis. Both the *c* axis excitation and the *b* axis excitation produce the highly *a* polarized emissions, even though the emission intensities and spectral profiles of the relevant emissions are considerably different (see Figs. 4 and 5). We infer from this fact that this strongly *a* axis polarized feature is common to the measurements in the stronger excitation regime.

The SNE is efficiently caused by the *c* axis polarized excitation. In particular, both the emission intensity and linewidth of the 507 nm line is very sensitive to the *c* polarized excitation energy. This line becomes strong and narrowed with increasing excitation energies (see Fig. 3). The intensity of the SNE is almost isotropic with the radial directions along the flat crystal plane paralleling the *bc* plane (Fig. 6). The *b* polarized excitation, however, turned out to be less effective in causing the SNE (Figs. 5 and 7). The 514 nm line intensity appears insensitive to excitation energies regardless of the excitation polarization direction. These observations indicate that the 507 nm line is solely responsible for the SNE. That the *c* axis excitation effectively causes the SNE, may be associated with the extension of π electrons in the molecules that is larger along the *c* axis than along the *b* axis.[20] The nature of the SNE is pertinent to the ASE which has been observed for other related materials of TPCOs.[14–17]

The isotropic feature of the SNE reflects the presence of the high gain media that comprise of molecules laterally packed in parallel with the crystal plane.[25]

V. CONCLUSION

We have carried out the polarized measurements of SNE with a single crystal of a TPCO of BP1T-OMe. The emissions from the crystal are strongly polarized along the *a* axis. Its polarization ratio of the *a* axis to the *b* axis was 16.7. This large ratio is due to the upright configuration of the molecular long axis that parallels the *a* axis. The emission spectra comprise of two major lines occurring at 507 and 514 nm. When the crystal is excited with the *c* axis polarized light, the SNE is definitively observed with an excitation threshold around a pulse laser energy of 300 $\mu J/cm^2$.

The intensity of the SNE is nearly isotropic with the radial directions along the flat crystal plane paralleling the *bc* plane. Of the two lines, the 507 nm line plays a major role in the SNE. Both its emission intensity and linewidth are very sensitive to the *c* polarized excitation energy. The 507 nm line becomes strong and narrowed with increasing excitation energies. The 514 nm line intensity, however, appears insensitive to excitation energies regardless of the excitation polarization direction. The *b* axis polarized excitation was less effective in causing the SNE.

ACKNOWLEDGMENTS

We thank Dr. Reiko Azumi, National Institute of Advanced Industrial Science and Technology (AIST), for her helpful discussions and suggestions on the crystal growth. This work was supported by a Grant-in-Aid for Science Research in a Priority Area "Super-Hierarchical Structures" (No. 17067009) from the Ministry of Education, Culture, Sports, Science and Technology, Japan.

[1] R. Gupta, M. Stevenson, A. Dogariu, M. D. McGehee, J. Y. Park, V. Srdanov, A. J. Heeger, and H. Wang, Appl. Phys. Lett. **73**, 3492 (1998).
[2] V. G. Kozlov, V. Bulović, P. E. Burrows, and S. R. Forrest, Nature **389**, 362 (1997).
[3] A. L. Briseno, R. J. Tseng, M.-M. Ling, E. H. L. Falcao, Y. Yang, F. Wudl, and Z. Bao, Adv. Mater. (Weinheim, Ger.) **18**, 2320 (2006).
[4] V. C. Sundar, J. Zaumseil, V. Podzorov, E. Menard, R. L. Willett, T. Someya, M. E. Gershenson, and J. A. Rogers, Science **303**, 1644 (2004).
[5] E. Menard, V. Podzorov, S.-H. Hur, A. Gaur, M. E. Gershenson, and J. A. Rogers, Adv. Mater. (Weinheim, Ger.) **16**, 2097 (2004).
[6] V. Podzorov, E. Menard, A. Borissov, V. Kiryukhin, J. A. Rogers, and M. E. Gershenson, Phys. Rev. Lett. **93**, 086602 (2004).
[7] R. Zeis, T. Siegrist, and Ch. Kloc, Appl. Phys. Lett. **86**, 022103 (2005).
[8] K. Nakamura, M. Ichikawa, R. Fushiki, T. Kamikawa, M. Inoue, T. Koyama, and Y. Taniguchi, Jpn. J. Appl. Phys., Part 2 **44**, L1367 (2005).
[9] K. Nakamura, M. Ichikawa, R. Fushiki, T. Kamikawa, M. Inoue, T. Koyama, and Y. Taniguchi, Jpn. J. Appl. Phys., Part 2 **43**, L100 (2004).
[10] M. Ichikawa, H. Yanagi, Y. Shimizu, S. Hotta, N. Suganuma, T. Koyama, and Y. Taniguchi, Adv. Mater. (Weinheim, Ger.) **14**, 1272 (2002).
[11] M. Mas-Torrent, M. Durkut, P. Hadley, X. Ribas, and C. Rovira, J. Am. Chem. Soc. **126**, 984 (2004).
[12] D. Fichou, S. Delysse, and J.-M. Nunzi, Adv. Mater. (Weinheim, Ger.) **9**, 1178 (1997).
[13] G. Horowitz, P. Valat, F. Garnir, F. Kouki, and V. Wintgens, Opt. Mater. (Amsterdam, Neth.) **9**, 46 (1998).
[14] M. Nagawa, R. Hibino, S. Hotta, H. Yanagi, M. Ichikawa, T. Koyama, and Y. Taniguchi, Appl. Phys. Lett. **80**, 544 (2002).
[15] R. Hibino, M. Nagawa, S. Hotta, M. Ichikawa, T. Koyama, and Y. Taniguchi, Adv. Mater. (Weinheim, Ger.) **14**, 119 (2002).
[16] M. Ichikawa, R. Hibino, M. Inoue, T. Haritani, S. Hotta, T. Koyama, and Y. Taniguchi, Adv. Mater. (Weinheim, Ger.) **15**, 213 (2003).
[17] K. Shimizu, D. Hoshino, and S. Hotta, Appl. Phys. Lett. **83**, 4494 (2003).
[18] M. Ichikawa, R. Hibino, M. Inoue, T. Haritani, S. Hotta, K. Araki, T. Koyama, and Y. Taniguchi, Adv. Mater. (Weinheim, Ger.) **17**, 2073 (2005).
[19] K. Shimizu, Y. Mori, and S. Hotta, J. Appl. Phys. **99**, 063505 (2006).
[20] S. Hotta, M. Goto, and R. Azumi, Chem. Lett. (Jpn.) **36**, 270 (2007).
[21] T. Katagiri and S. Hotta, J. Heterocyclic Chem. (to be published).
[22] R. Azumi, M. Goto, K. Honda, and M. Matsumoto, Bull. Chem. Soc. Jpn. **76**, 1561 (2003).
[23] T. Yamao, Y. Kawasaki, S. Ota, S. Hotta, and R. Azumi, Macromol. Symp. **242**, 315 (2006).
[24] T-H. Kim, J. H. Lee, J. H. Kim, and C. Seoul, Mater. Res. Soc. Symp. Proc. **920**, 0920–S02–04 (2006).
[25] A. E. Siegman, *Lasers* (University Science Books, Sausalito, 1986), Chap. 13.